

Electronic Supplementary Information

Supramolecular Assembly of Chiral Polyoxometalate Complexes for Asymmetric Catalytic Oxidation of Thioethers

Yizhan Wang, Haolong Li, Wei Qi, Yang Yang, Yi Yan, Bao Li, and Lixin Wu*

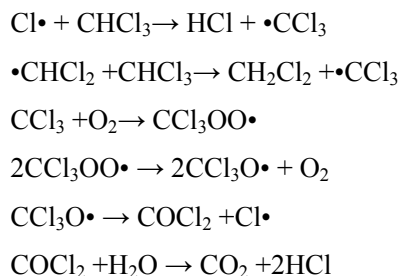
State Key Laboratory of Supramolecular Structure and Materials, College of Chemistry, Jilin University,

Changchun 130012, P. R. China

E-mail: wulx@jlu.edu.cn; Fax: +86 431 85193421; Tel: +86 431 85168481

The safety concerning the phosgene formation in the reaction system

The chloroform is normally prone to produce phosgene under the presence of peroxide under heating or light radiation.¹ When chloroform decomposes in the presence of air under the exposure to UV light (<260 nm), a complex sequence of reactions lead eventually to the production of CO₂ and HCl. According to the reported data,² the following steps would happen:



In our experiments, the oxidation with hydrogen peroxide (30%) in a biphasic mixture of water and chloroform is carried out at 0 °C in dark place. The commercially acquired chloroform is used without further purification. In case of that the COCl₂ formed in the biphasic mixture of water and chloroform, HCl and CO₂ could be predicted due to the hydrolysis in water. Therefore, we used the 0.1 M AgNO₃ to detect the possible chloride ion in the water phase. Similar to the published results, no precipitation was found (Fig. S45). We also tested the possible phosgene by using filter paper (treated with 5% diphenylamine, 5% dimethylaminobenzaldehyde in alcohol, and then dried), and no COCl₂ was detected (Fig. S46). So, the present reaction condition is quite safe. In contrast to the catalytic condition, the production of COCl₂ is unavoidable when the reaction system is heated or exposed in UV light. Therefore, any exposure to the UV light and heating of the present catalytic system must be prohibited.

Additional Characterization

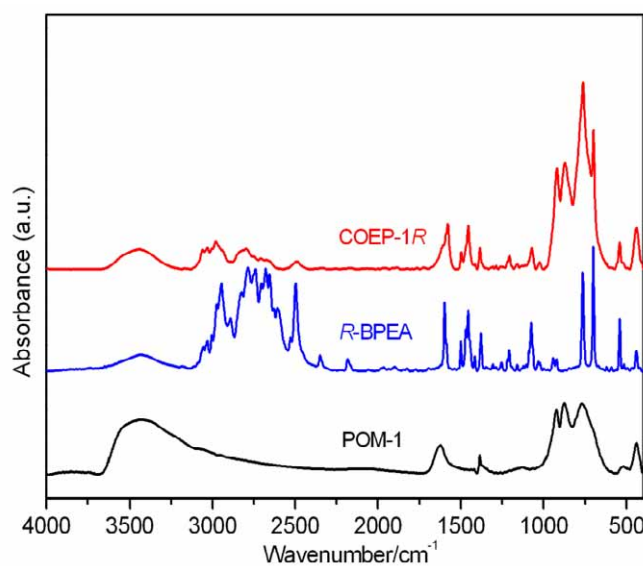


Figure S1. IR spectra of POM-1 ($\text{Na}_{12}[\text{WZn}_3(\text{H}_2\text{O})_2(\text{ZnW}_9\text{O}_{34})_2]\cdot46\text{H}_2\text{O}$) (bottom), *R*-BPEA (middle) and COEP-1*R* (top) in KBr pellets.

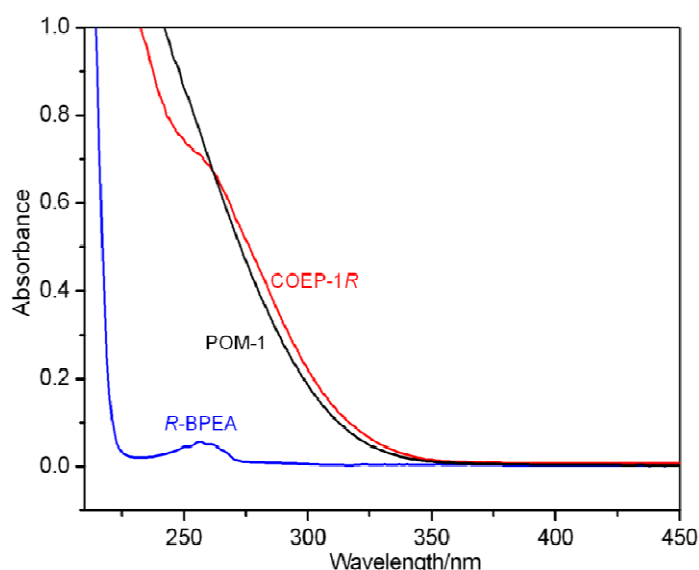


Figure S2. UV-Vis spectra of POM-1 ($\text{Na}_{12}[\text{WZn}_3(\text{H}_2\text{O})_2(\text{ZnW}_9\text{O}_{34})_2]\cdot46\text{H}_2\text{O}$) (black), *R*-BPEA (blue) and COEP-1*R* (red) in CH_3CN .

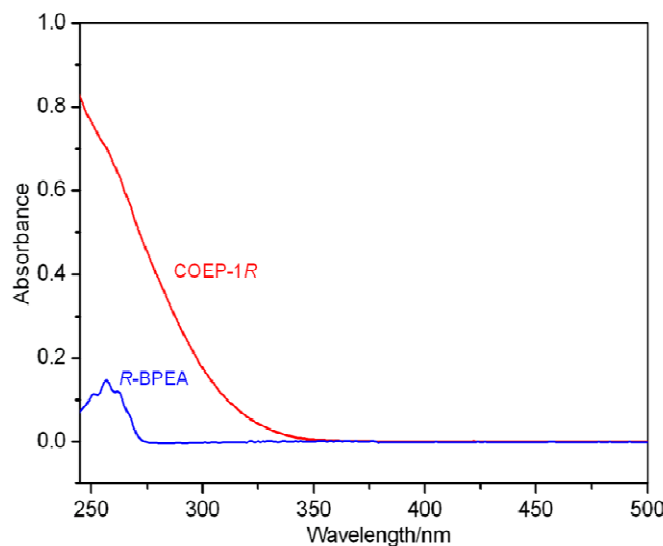


Figure S3. UV-Vis spectra of *R*-BPEA (blue) and COEP-1*R* (red) in CH_2Cl_2 .

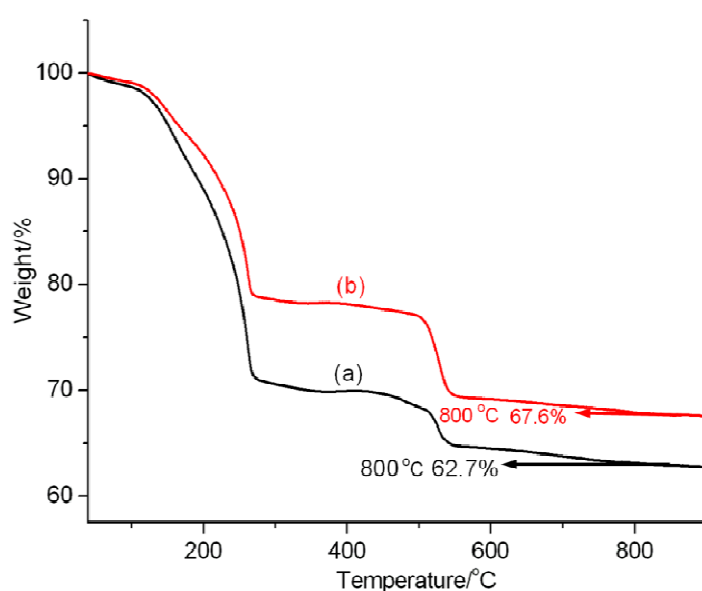


Figure S4. TGA curves of (a) the original COEP-1*R* and (b) the recoverd COEP-1*R*, in which the experiment is carried out in air with a heating rate of $10\text{ }^{\circ}\text{C min}^{-1}$.

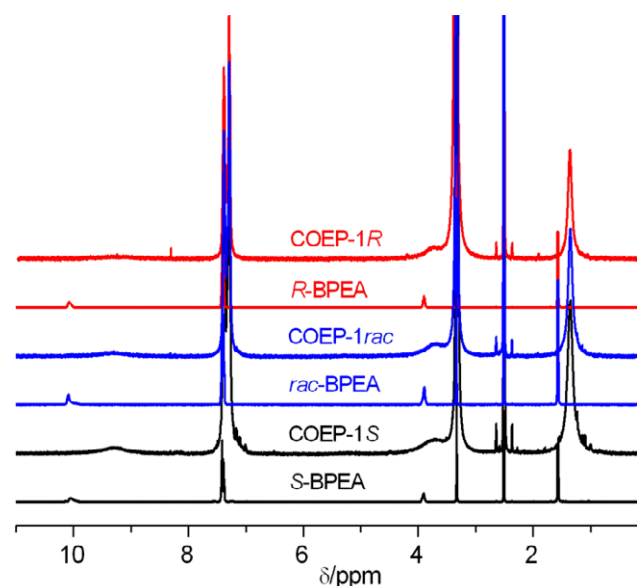


Figure S5. ^1H NMR spectra of COEP-1*R*, COEP-1*S* and COEP-1*rac* in $\text{DMSO}-d^6$.

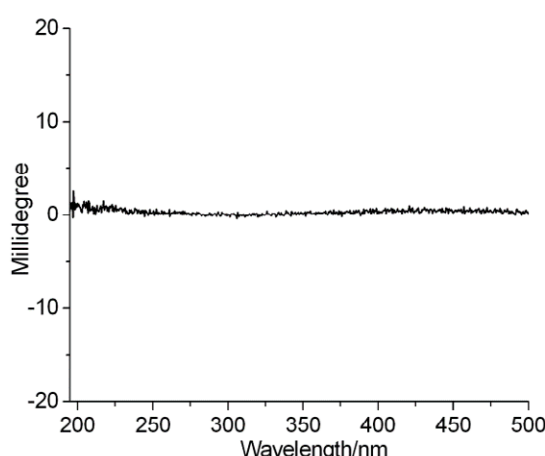


Figure S6. CD spectra of COEP-1*rac* in CH_3CN at concentration of $2.6 \times 10^{-5} \text{ mol L}^{-1}$.

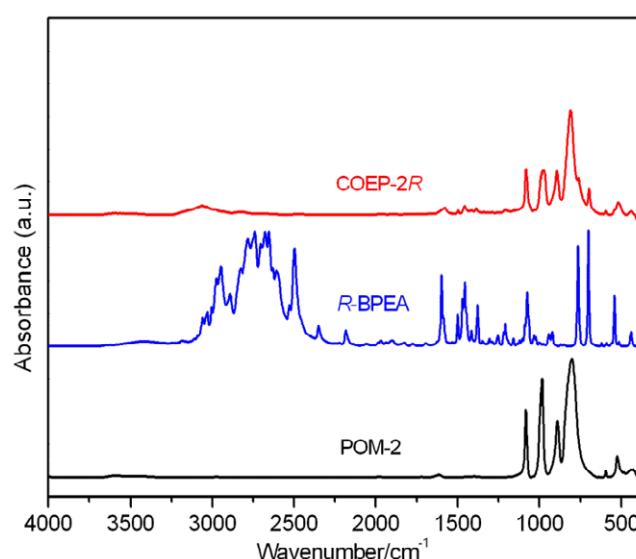


Figure S7. IR spectra of POM-2 ($\text{H}_3\text{PW}_{12}\text{O}_{40}$) (bottom), R-BPEA (middle) and COEP-2*R* (top) in KBr pellets.

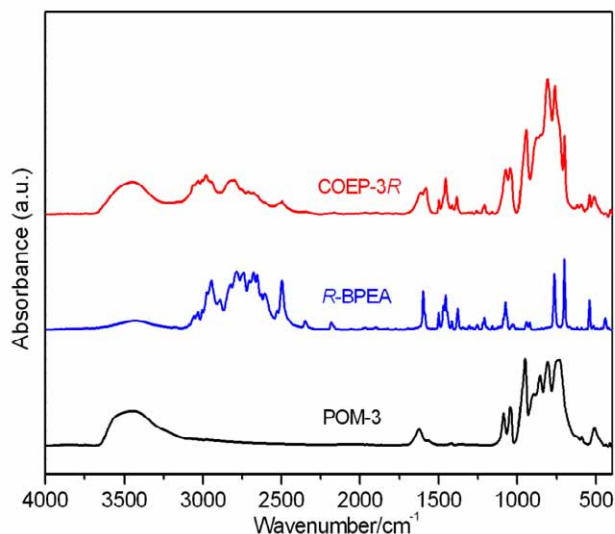


Figure S8. IR spectra of POM-3 ($K_7PW_{11}O_{39}\cdot12H_2O$) (bottom), *R*-BPEA (middle) and COEP-3*R* (top) in KBr pellets.

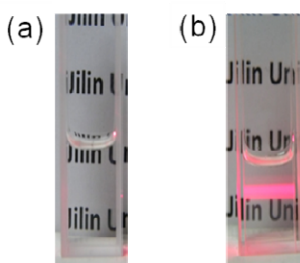


Figure S9. Digital photographs of COEP-1*R* (0.4 μ mol) in the reaction system for methyl phenyl sulfide (0.4 mmol) oxidation in $CHCl_3$ (2 mL) (a) without and (b) with addition of the H_2O_2 (30%, 0.4 mmol) at RT.

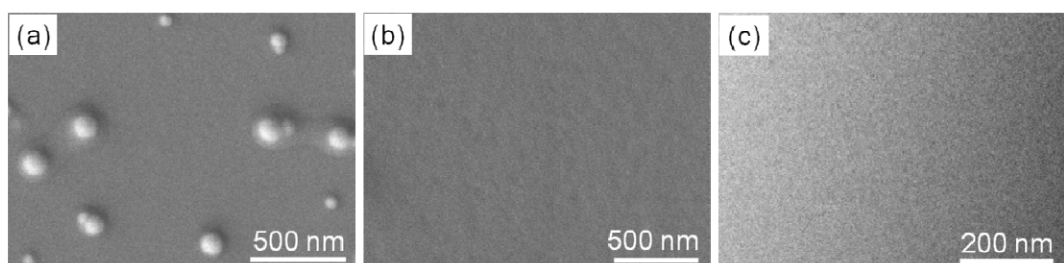


Figure S10. (a), (b) SEM and (c) TEM images of COEP-1*R* (0.4 μ mol) in $CHCl_3$ (2 mL) solution containing methyl phenyl sulfide (0.4 mmol) at RT, where (a) with and (b), (c) without addition of oxidant H_2O_2 (30%, 0.4 mmol).

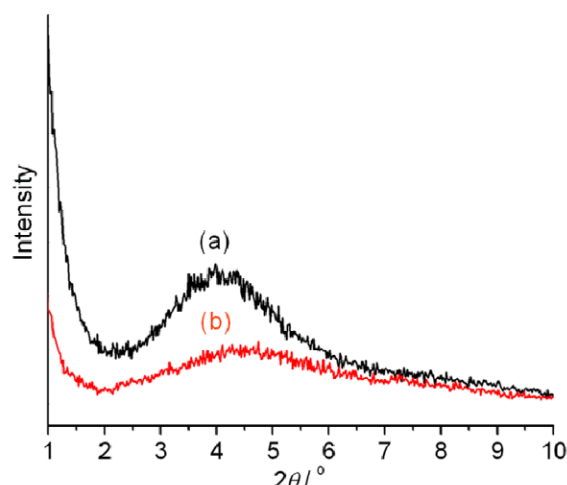


Figure S11. XRD pattern of COEP-1*R* before (a) and after (b) assembly in $CHCl_3$ at RT.

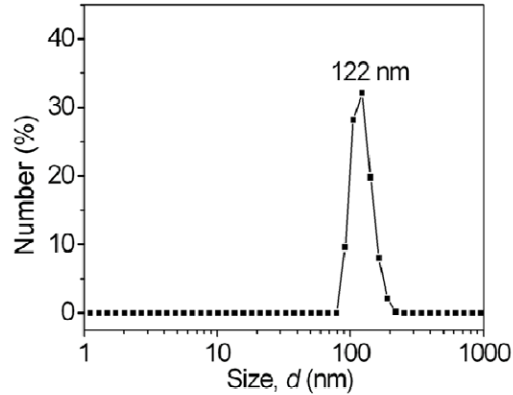


Figure S12. DLS plot of COEP-1*R* reaction solution for methyl phenyl sulfide oxidation after the reaction finished. Reaction conditions: methyl phenyl sulfide (0.4 mmol), H₂O₂ (30%, 0.4 mmol), COEP-1*R* (0.4 μmol), CHCl₃ (2 mL), RT.

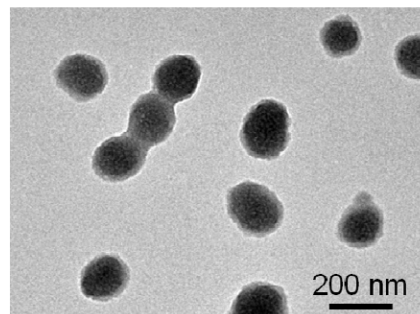


Figure S13. TEM images of COEP-3*R* assemblies in the reaction solution of methyl phenyl sulfide oxidation in CHCl₃.

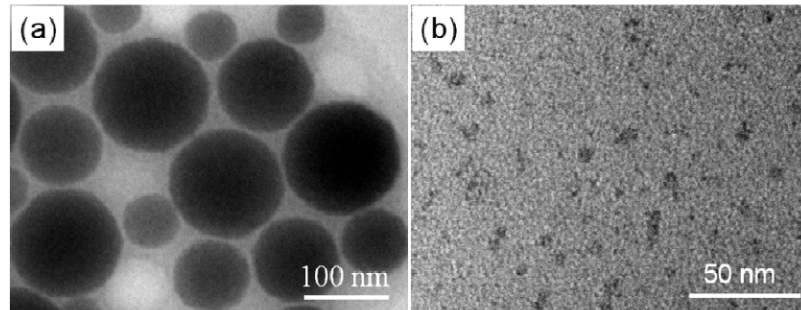


Figure S14. TEM images of COEP-1*R* assemblies in the reaction solution of methyl phenyl sulfide oxidation in (a) CHCl₃ and (b) CH₃CN.

Table S1. The coverage density summary of stereocenters on POM surface of COEP-2*R*, COEP-3*R* and COEP-1*R*.

	COEP-2 <i>R</i> (C ₁₆ H ₂₀ N) ₃ PW ₁₂ O ₄₀	COEP-3 <i>R</i> (C ₁₆ H ₂₀ N) ₆ KPW ₁₁ O ₃₉	COEP-1 <i>R</i> (C ₁₆ H ₂₀ N) ₁₂ WZn ₃ (ZnW ₉ O ₃₄) ₂
Surface area of POM	S	~S	~1.7S
Number of stereocenter	6	12	24
Coverage density	6/S	~12/S	~14/S

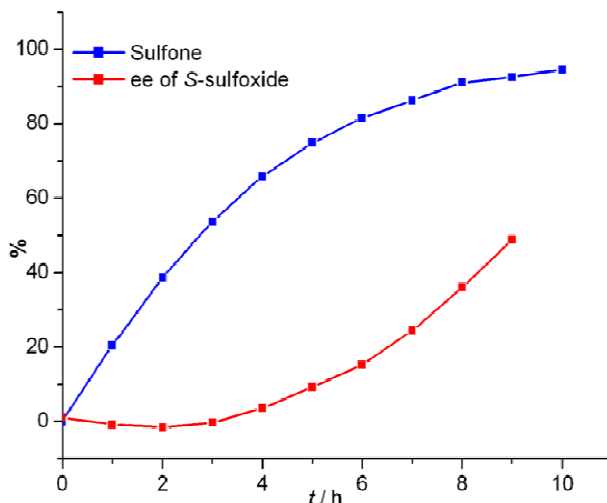


Figure S15. Time profiles of the oxidaion of racemic methyl phenyl sulfoxide (0.4 mmol) with H₂O₂ (30%, 0.4 mmol) using COEP-1S (0.4 μmol) as asymmetric catalyst in CHCl₃ (2 mL) at 0 °C.

Table S2. The summary of reuse COEP-1R for asymmetric catalytic oxidation of methyl phenyl sulfide.^[a]

Entry	Isolated Yield	Conversion ^[b]	SO:SO ₂ (%) ^[c]	ee (%) ^[d]
1	80%	85%	96:4	18 (R)
2	78%	80%	97:3	16 (R)
3	75%	78%	95:5	13 (R)

[a] All reactions are performed with sulfide (0.4 mmol) in CHCl₃ (2 mL). [b] Conversion is determined by HPLC. [c] SO and SO₂ stand for the sulfoxide and the sulfone respectively. [d] The ee values are measured by HPLC analysis with a chiralcel OD-H column. The absolute configuration is determined by comparison of the HPLC results with the data in the literature.

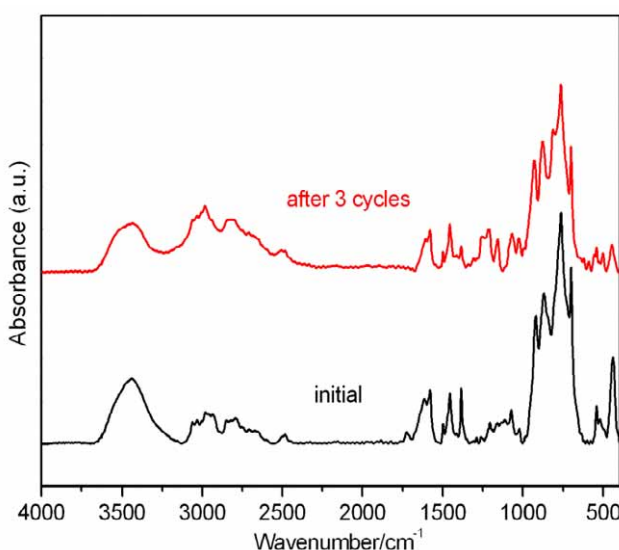


Figure S16. IR spectra of freshly prepared (bottom in black) and recovered (top in red) catalyst COEP-1R.

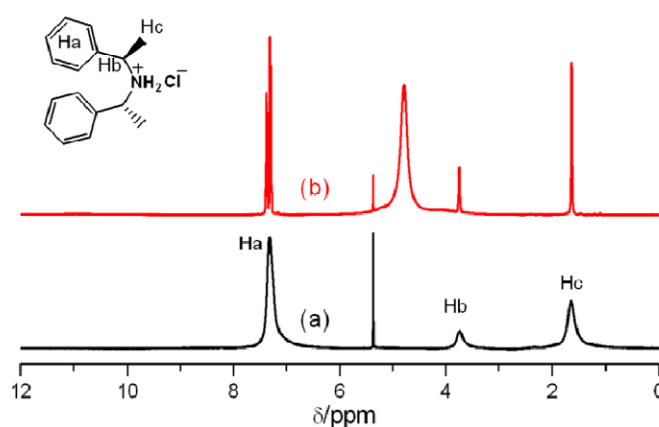


Figure S17. ¹H NMR spectra of (a) COEP-1R and (b) COEP-1R with H_2O_2 (mole ratio of COEP-1R: H_2O_2 = 1:500) in CD_2Cl_2 .

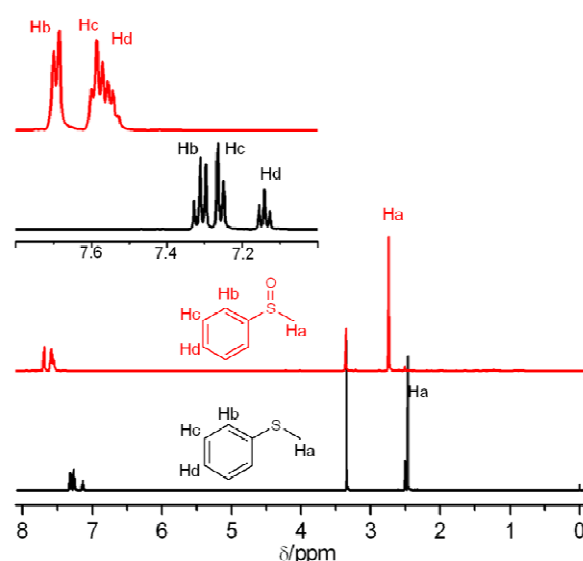


Figure S18. ¹H NMR spectra of methyl phenyl sulfide (bottom in black) and methyl phenyl sulfoxide (R, 40% ee) (top in red) in $\text{DMSO}-d_6$.

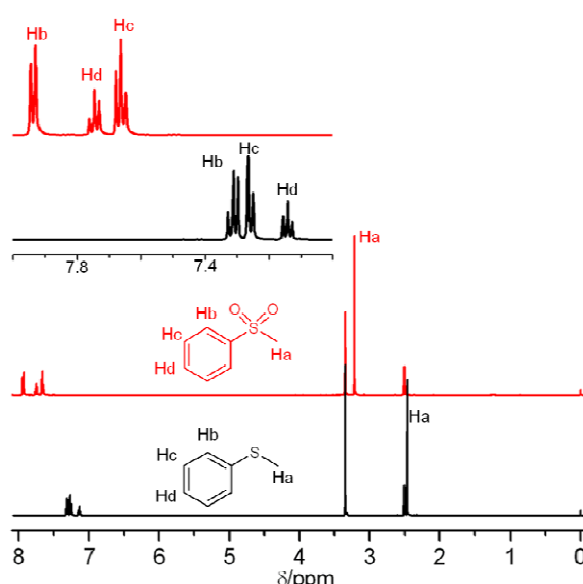


Figure S19. ¹H NMR spectra of methyl phenyl sulfide (bottom in black) and methyl phenyl sulfone (top in red) in $\text{DMSO}-d_6$.

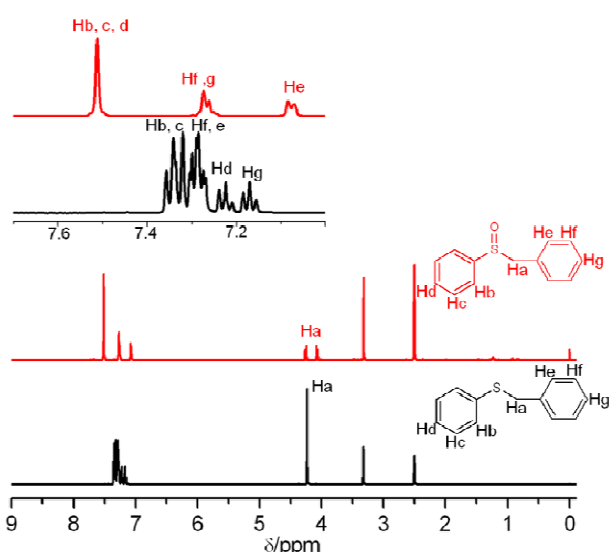


Figure S20. ¹H NMR spectra of benzyl phenyl sulfide (bottom in black) and benzyl phenyl sulfoxide (*R*, 51% ee) (top in red) in DMSO-*d*⁶.

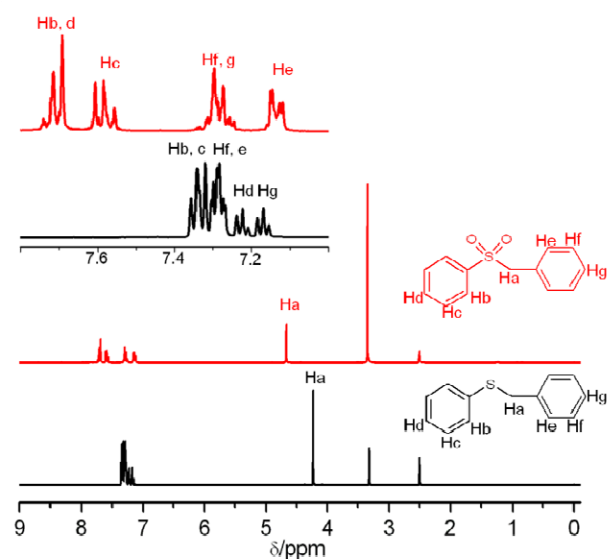


Figure S21. ¹H NMR spectra of benzyl phenyl sulfide (bottom in black) and benzyl phenyl sulfone (top in red) in DMSO-*d*⁶.

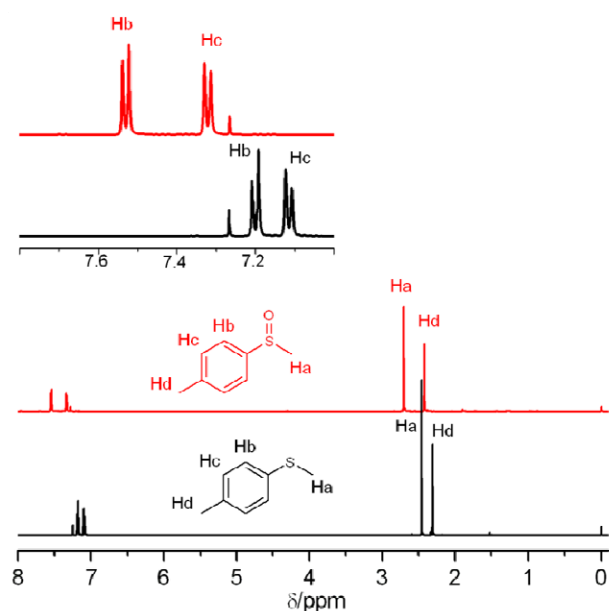


Figure S22. ^1H NMR spectra of methyl *p*-tolyl sulfide (bottom in black) and methyl *p*-tolyl sulfoxide (*R*, 53% ee) (top in red) in CDCl_3 .

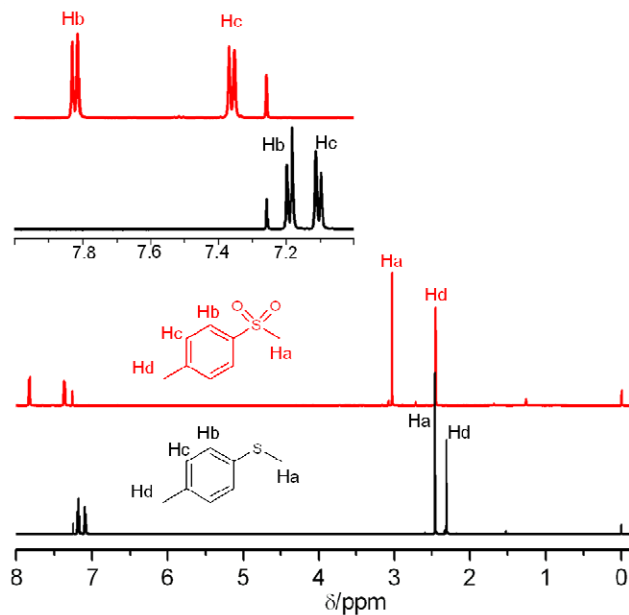


Figure S23. ^1H NMR spectra of methyl *p*-tolyl sulfide (bottom in black) and methyl *p*-tolyl sulfone (top in red) in CDCl_3 .

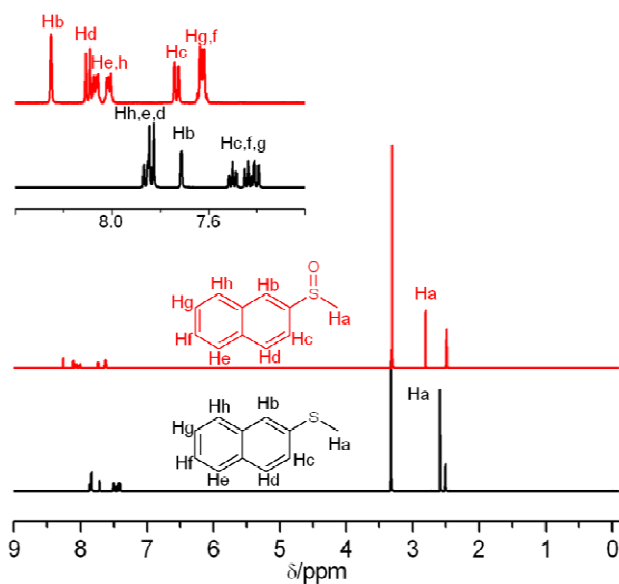


Figure S24. ^1H NMR spectra of 2-naphthyl methyl sulfide (bottom in black) and 2-naphthyl methyl sulfoxide (*R*, 35% ee) (top in red) in $\text{DMSO}-d_6$.

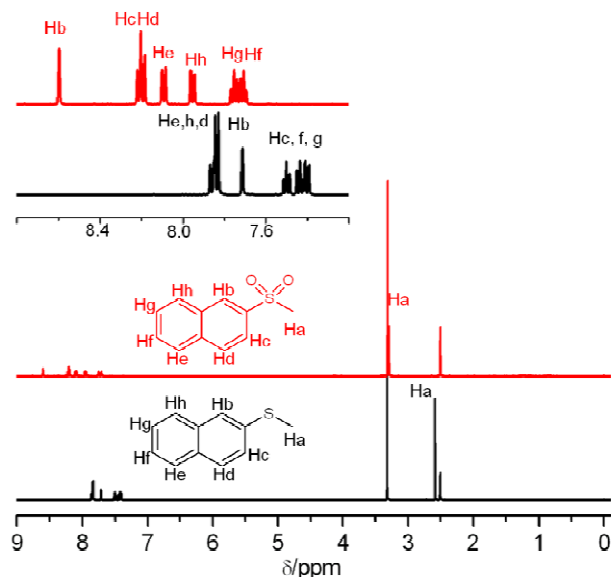


Figure S25. ¹H NMR spectra of 2-naphthyl methyl sulfide (bottom in black) and 2-naphthyl methyl sulfone (top in red) in DMSO-*d*⁶.

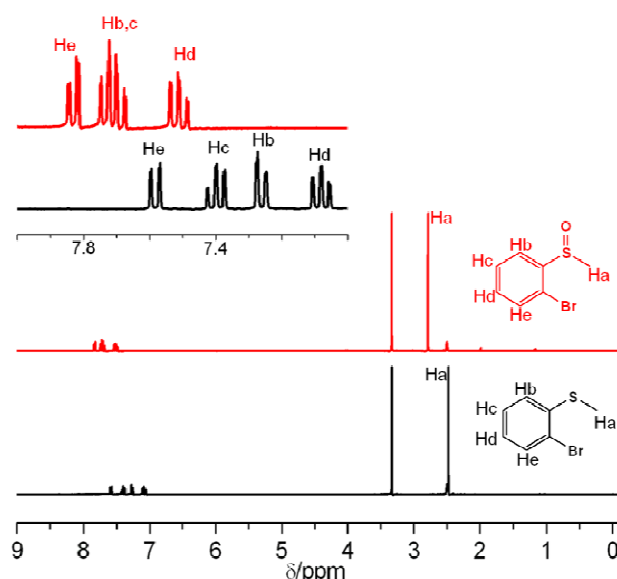


Figure S26. ¹H NMR spectra of 2-bromophenyl methyl sulfide (bottom in black) and 2-bromophenyl methyl sulfoxide (top in red) in DMSO-*d*⁶.

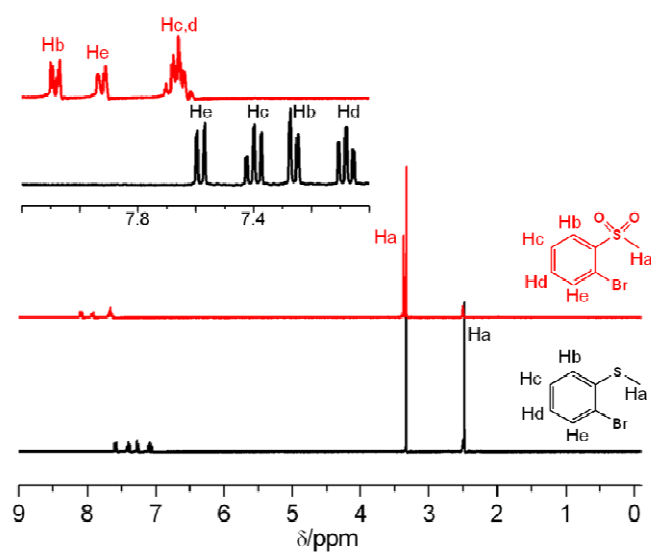


Figure S27. ^1H NMR spectra of 2-bromophenyl methyl sulfide (bottom in black) and 2-bromophenyl methyl sulfone (top in red) in $\text{DMSO}-d_6$.

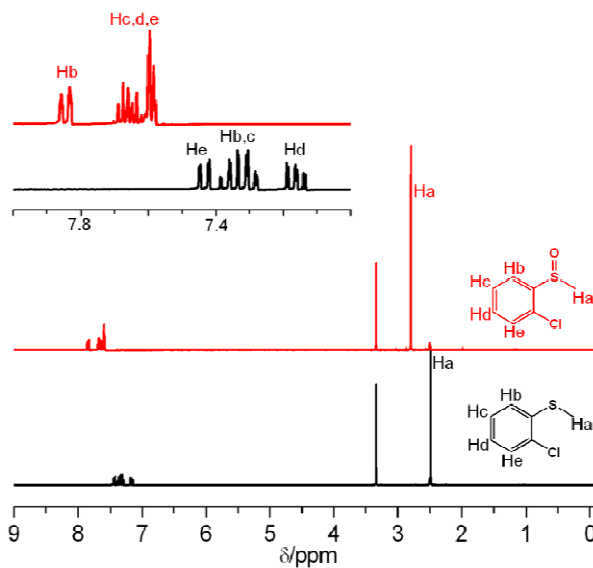


Figure S28. ^1H NMR spectra of 2-chlorophenyl methyl sulfide (bottom in black) and 2-chlorophenyl methyl sulfoxide (top in red) in $\text{DMSO}-d_6$.

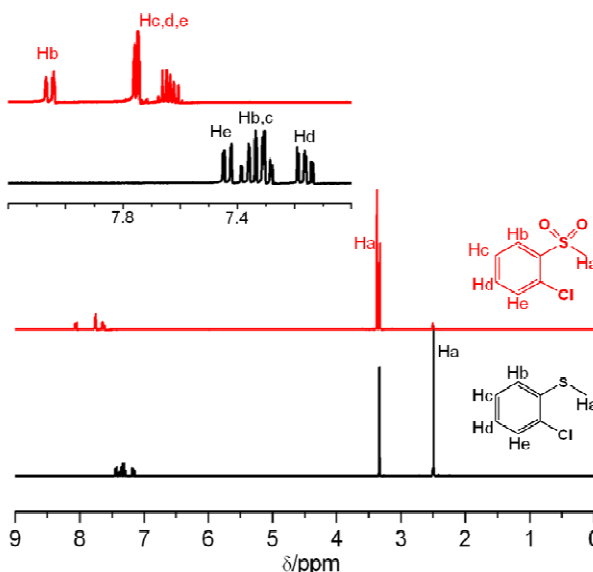


Figure S29. ^1H NMR spectra of 2-chlorophenyl methyl sulfide (bottom in black) and 2-chlorophenyl methyl sulfone (top in red) in $\text{DMSO}-d_6$.

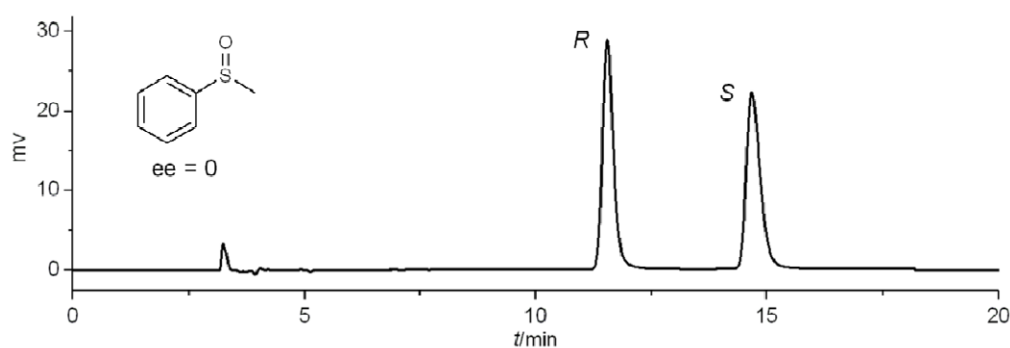


Figure S30. HPLC plot of racemic methyl phenyl sulfoxide under the conditions of chiralcel OD-H, flow rate: $1.0 \text{ mL}\cdot\text{min}^{-1}$, hexane/iPrOH = 90/10, and wavelength: 254 nm. Retention time: $t_1(R) = 11.55 \text{ min}$, $t_2(S) = 14.68 \text{ min}$.

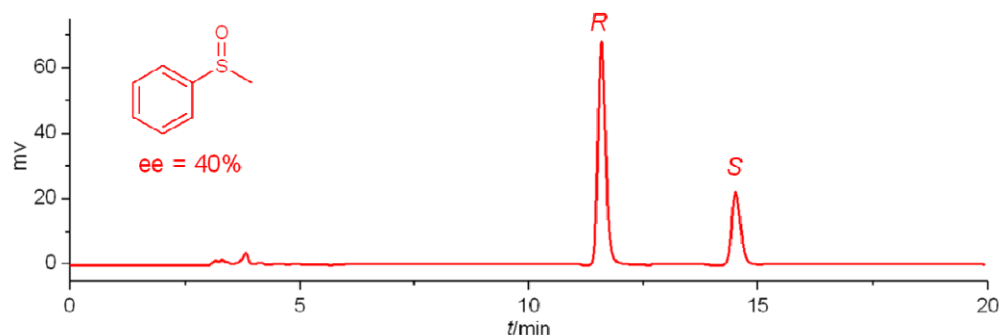


Figure S31. HPLC plot of methyl phenyl sulfoxide (*R*, 40% ee) under the conditions of chiralcel OD-H, flow rate: 1.0 $\text{mL}\cdot\text{min}^{-1}$, hexane/iPrOH = 90/10, and wavelength: 254 nm. Retention time: t_1 (*R*) = 11.58 min, t_2 (*S*) = 14.50 min.

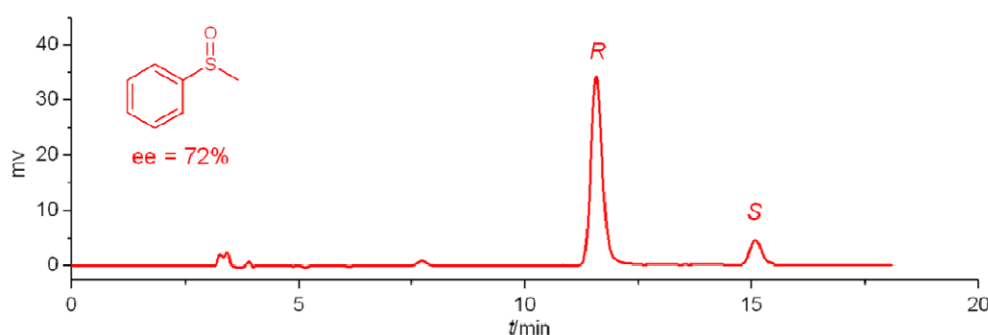


Figure S32. HPLC plot of methyl phenyl sulfoxide (*R*, 72% ee) under the conditions of chiralcel OD-H, flow rate: 1.0 $\text{mL}\cdot\text{min}^{-1}$, hexane/iPrOH = 90/10, and wavelength: 254 nm. Retention time: t_1 (*R*) = 11.56 min, t_2 (*S*) = 15.09 min.

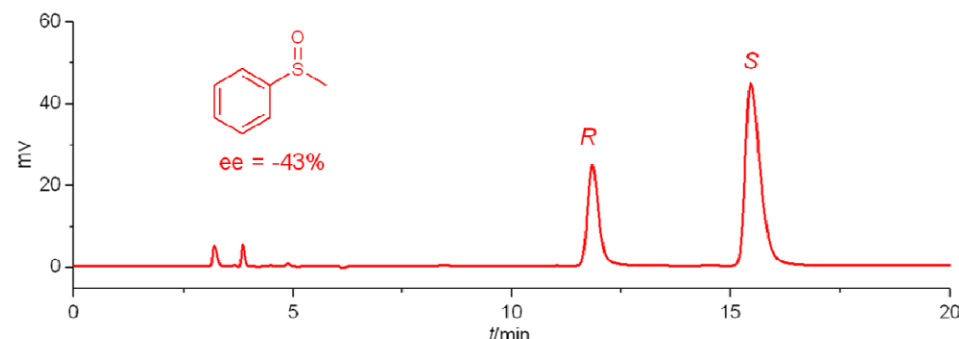


Figure S33. HPLC plot of methyl phenyl sulfoxide (*S*, -43% ee) under the conditions of chiralcel OD-H, flow rate: 1.0 $\text{mL}\cdot\text{min}^{-1}$, hexane/iPrOH = 90/10, and wavelength: 254 nm. Retention time: t_1 (*R*) = 11.84 min, t_2 (*S*) = 15.46 min.

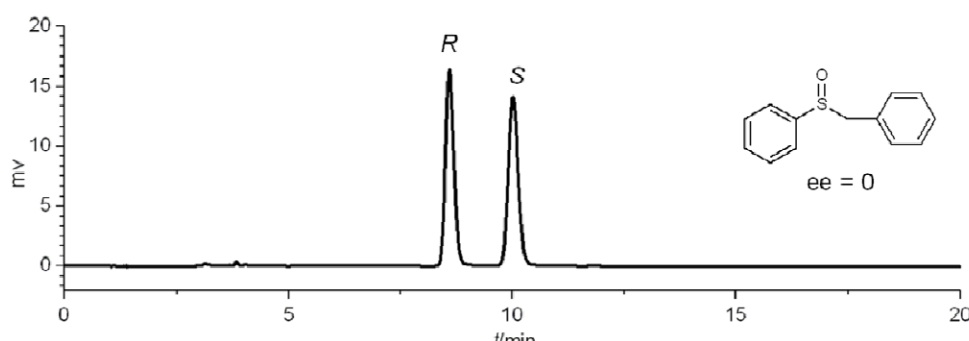


Figure S34. HPLC plot of racemic benzyl phenyl sulfoxide under the conditions of chiralcel OD-H, flow rate: 1.0 $\text{mL}\cdot\text{min}^{-1}$, hexane/iPrOH = 80/20, and wavelength: 254 nm. Retention time: t_1 (*R*) = 8.60 min, t_2 (*S*) = 10.01 min.

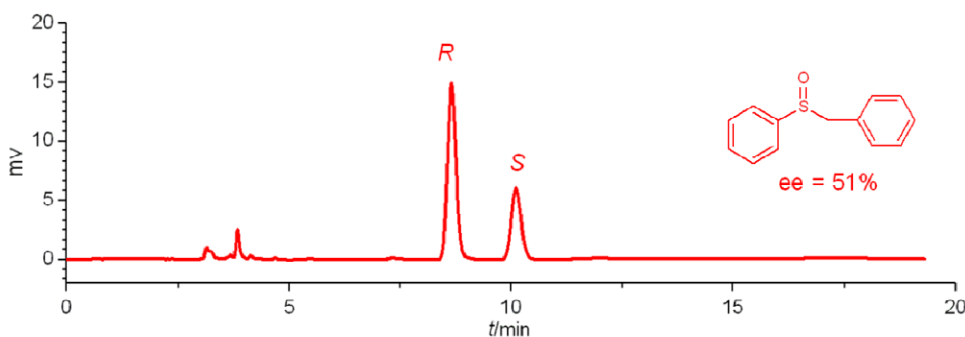


Figure S35. HPLC plot of benzyl phenyl sulfoxide (*R*, 51% ee) under the conditions of chiralcel OD-H, flow rate: 1.0 mL·min⁻¹, hexane/iPrOH = 80/20, and wavelength: 254 nm. Retention time: t₁ (*R*) = 8.65 min, t₂ (*S*) = 10.11 min.

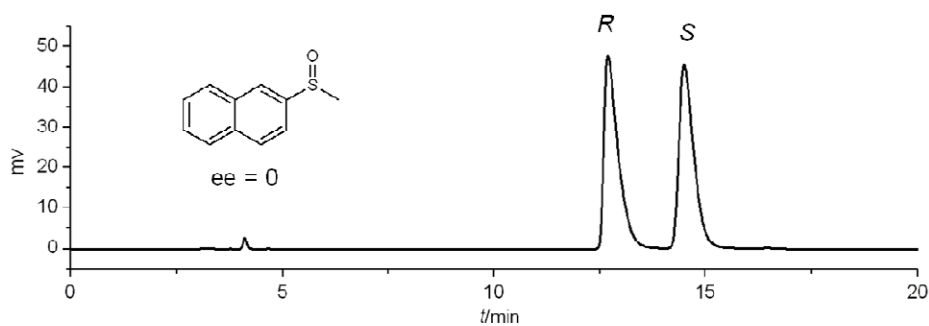


Figure S36. HPLC plot of racemic 2-naphthyl methyl sulfoxide under the conditions of chiralcel OD-H, flow rate: 1.0 mL·min⁻¹, hexane/iPrOH = 85/15, and wavelength: 254 nm. Retention time: t₁ (*R*) = 12.70 min, t₂ (*S*) = 14.50 min.

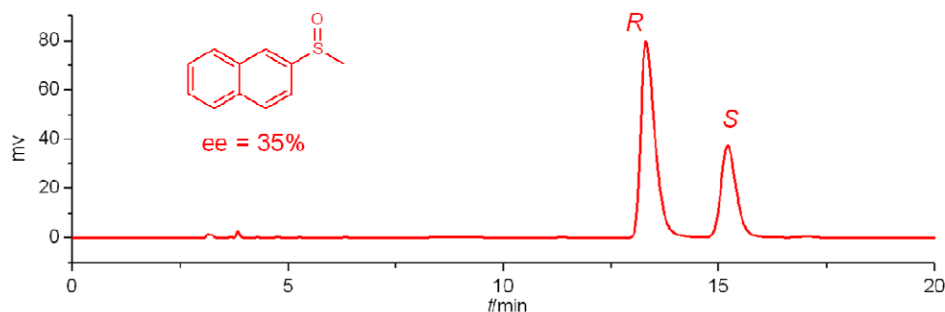


Figure S37. HPLC plot of 2-naphthyl methyl sulfoxide (*R*, 35% ee) under the conditions of chiralcel OD-H, flow rate: 1.0 mL·min⁻¹, hexane/iPrOH = 85/15, and wavelength: 254 nm. Retention time: t₁ (*R*) = 13.31 min, t₂ (*S*) = 15.21 min.

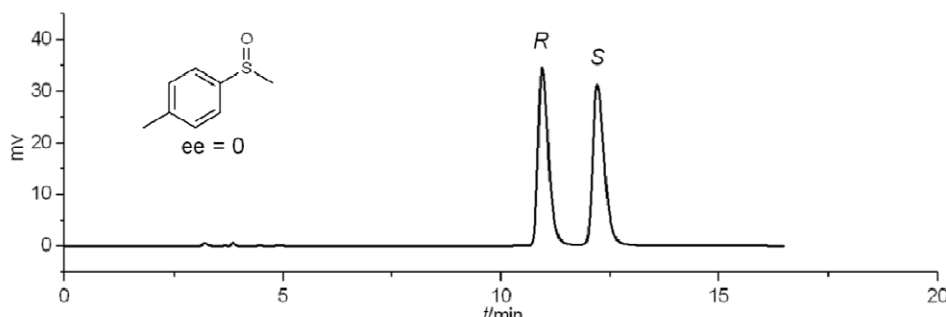


Figure S38. HPLC plot of racemic methyl *p*-tolyl sulfoxide under the conditions of chiralcel OD-H, flow rate: 1.0 mL·min⁻¹, hexane/iPrOH = 90/10, and wavelength: 254 nm. Retention time: t₁ (*R*) = 10.94 min, t₂ (*S*) = 12.21 min.

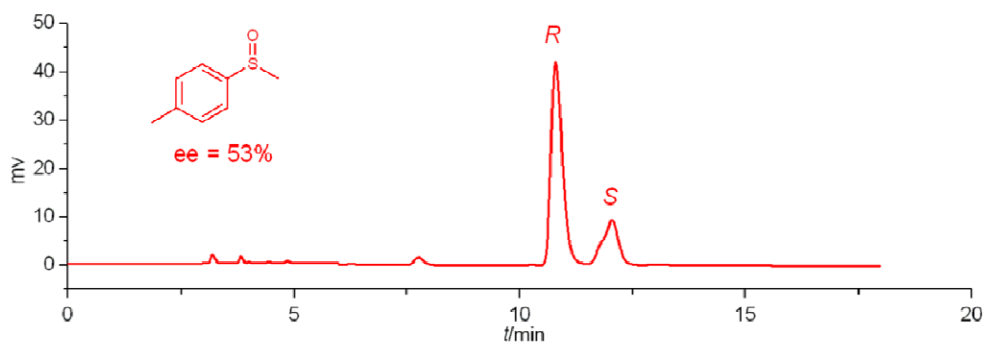


Figure S39. HPLC plot of methyl *p*-tolyl sulfoxide (*R*, 53% ee) under the conditions of chiralcel OD-H, flow rate: 1.0 $\text{mL}\cdot\text{min}^{-1}$, hexane/*i*PrOH = 90/10, and wavelength: 254 nm. Retention time: $t_1(R) = 10.79 \text{ min}$, $t_2(S) = 12.04 \text{ min}$.

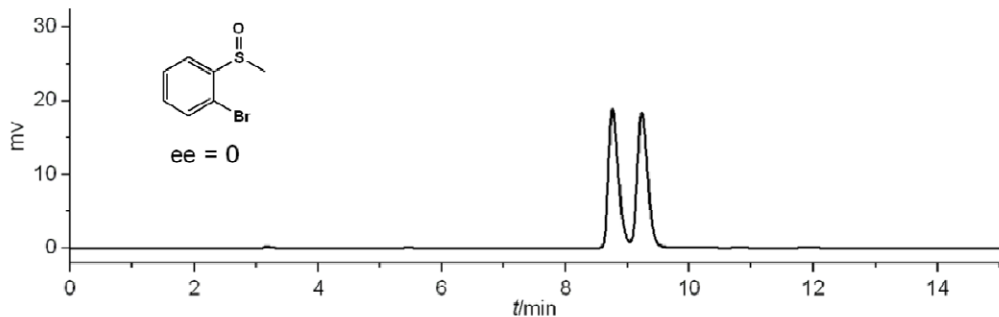


Figure S40. HPLC plot of racemic 2-bromophenyl methyl sulfoxide under the conditions of chiralcel OD-H, flow rate: 1.0 $\text{mL}\cdot\text{min}^{-1}$, hexane/*i*PrOH = 90/10, and wavelength: 254 nm. Retention time: $t_1 = 8.76 \text{ min}$, $t_2 = 9.23 \text{ min}$.

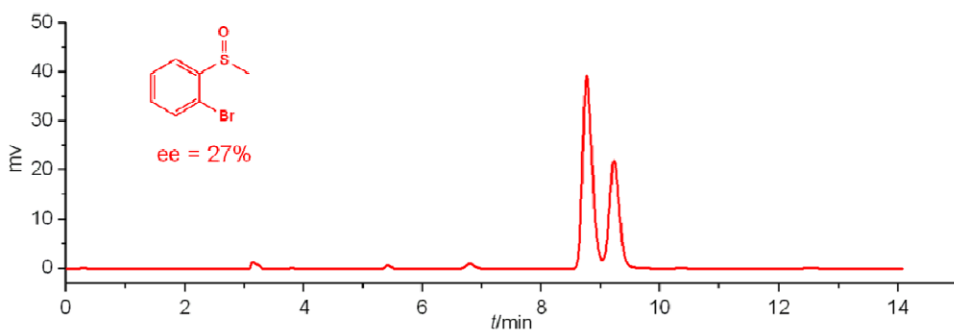


Figure S41. HPLC plot of 2-bromophenyl methyl sulfoxide (27% ee) under the conditions of chiralcel OD-H, flow rate: 1.0 $\text{mL}\cdot\text{min}^{-1}$, hexane/*i*PrOH = 90/10, and wavelength: 254 nm. Retention time: $t_1 = 8.76 \text{ min}$, $t_2 = 9.23 \text{ min}$.

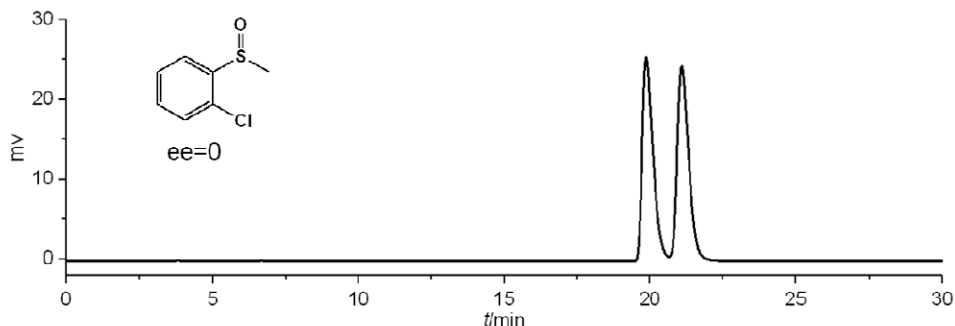


Figure S42. HPLC plot of racemic 2-chlorophenyl methyl sulfoxide under the conditions of chiralcel OD-H, flow rate: 1.0 $\text{mL}\cdot\text{min}^{-1}$, hexane/*i*PrOH = 98/2, and wavelength: 254 nm. Retention time: $t_1 = 19.87 \text{ min}$, $t_2 = 21.08 \text{ min}$.

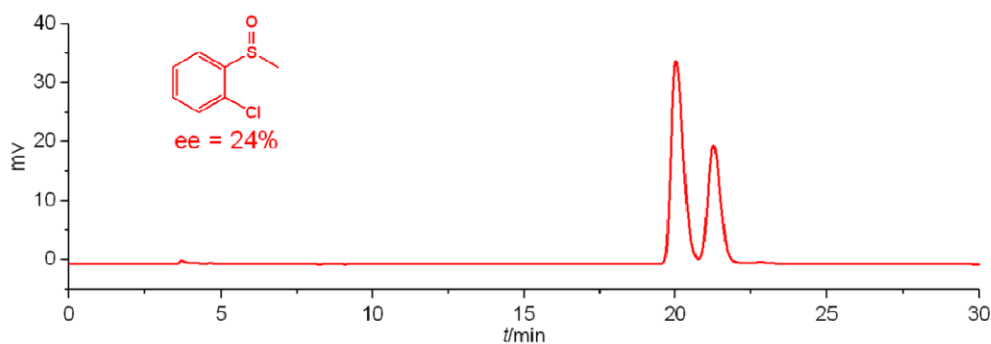


Figure S43. HPLC plot of 2-chlorophenyl methyl sulfoxide (24% ee) under the conditions of chiralcel OD-H, flow rate: 1.0 $\text{mL}\cdot\text{min}^{-1}$, hexane/iPrOH = 98/2, and wavelength: 254 nm. Retention time: $t_1 = 20.02 \text{ min}$, $t_2 = 21.25 \text{ min}$.

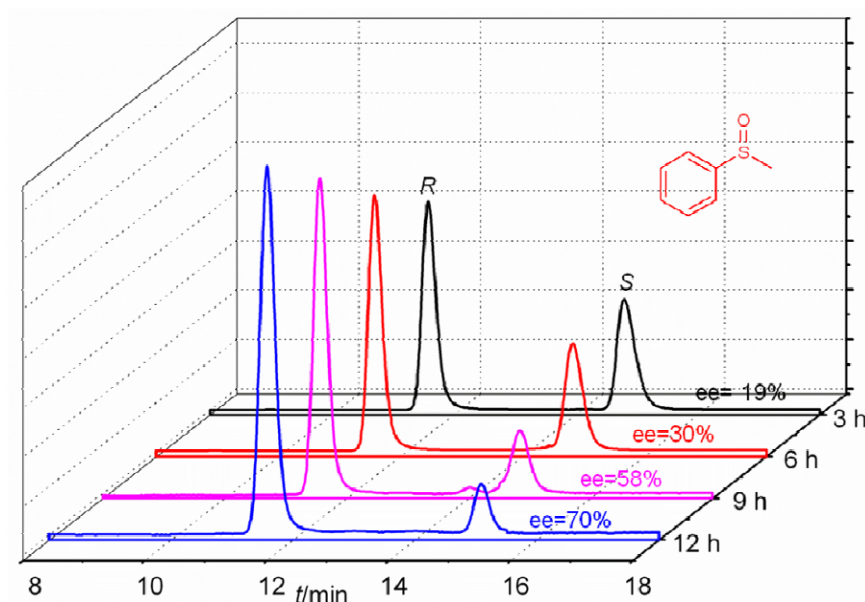


Figure S44. The HPLC diagrams for the oxidation of methyl phenyl sulfide (0.4 mmol) with H_2O_2 (30%, 1.0 mmol), using COEP-1R (0.4 μmol) as asymmetric catalyst in CHCl_3 (2 mL) at 0 $^\circ\text{C}$.

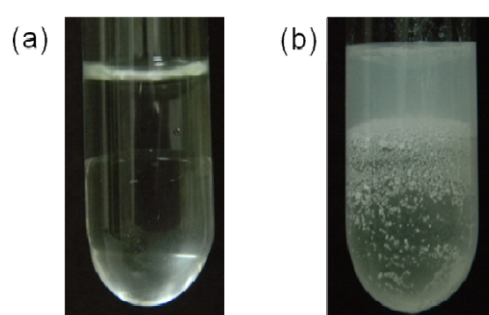


Figure S45. Digital photographs for (a) the reaction solution of methyl phenyl sulfide oxidation after the reaction is carried out for 24 hours and (b) the control mixture of 2 mL CHCl_3 and 0.1 mL H_2O_2 (30%) encountering a UV irradiation for 10 min with addition of 0.1 M AgNO_3 .

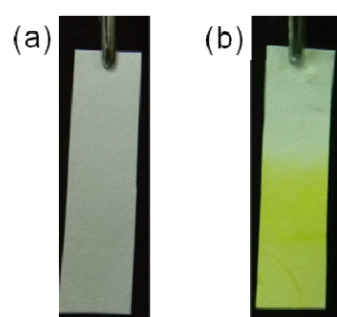


Figure S46. Digital photographs of the filter paper (treated with 5% diphenylamine and 5% dimethylaminobenzaldehyde in alcohol, and then dried) after treating with (a) the reaction system of methyl phenyl sulfide oxidation during the reaction process, and (b) CHCl₃ exposing in the UV light.

References:

1. A. Alippi, F. Cataldo and A. Galbato, *Ultrasonics*, **1992**, *30*, 148.
2. L. A. Peña and P. E. Hoggard, *J. Mol. Catal. A: Chem.*, **2010**, *327*, 20.